Reconstruction of unbroken vasculature of mouse by varying the slope of the scan plane in MRI

You may also be interested in:

Physical considerations in using thermal techniques for the delineation of radiation damage in skin
J O Fenn, C J Klobukowski, E A Travis et al.

Endovascular interventional magnetic resonance imaging
L W Bartels and C J G Bakker

Diagnostic criteria for mass lesions differentiating in electrical impedance mammography
Karpov A and Korotkova M

Electrical impedance potential mammography for visualization of objects (electrochemical tests)
A Karpov, M Korotkova, Yu Tsofin et al.

An automated system for ultrasound scanner evaluation usingPSF analysis of received signal
L Dolezal, J Hálek, Ch Kollmann et al.

Using of electrical impedance tomography for diagnostics of the cervix uteri diseases
O V Trokhanova, Y A Chijova, M B Okhapkin et al.

Electric impedance imaging of the mammary gland in the case of mastitis
M Korotkova and A Karpov

Medical ultrasound: a new metric of performance for grey-scaleimaging
S D Pye, W Ellis and T MacGillivray

Formation of laser pulses by deflector system
V A Malinov and V N Chernov

Reconstruction of unbroken vasculature of mouse by varying the slope of the scan plane in MRI

S Maltseva[1,2,3], A Cherevko[2,3,4], A Khe[2,3,4], A Akulov[5,6], A Savelov[4], A Tulupov[3,4], E Derevtsov[1,3], M Moshkin[3,4,5], A Chupakhin[2,3,4]

[1]Sobolev Institute of Mathematics, Siberian Branch of the Russian Academy of Sciences, Novosibirsk, Russian Federation
[2]Lavrentyev Institute of Hydrodynamics, Siberian Branch of the Russian Academy of Sciences, Novosibirsk, Russian Federation
[3]Novosibirsk State University, Novosibirsk, Russian Federation
[4]International Tomography Center, Siberian Branch of the Russian Academy of Sciences, Novosibirsk, Russian Federation
[5]Cytology and Genetics Institute, Siberian Branch of the Russian Academy of Sciences, Novosibirsk, Russian Federation
[6] Neurobiology Lab, Research Institute of Biology and Biophysics, Tomsk State University, Tomsk, Russian Federation

E-mail: cherevko@mail.ru

Abstract. Reconstruction of vascular net of small laboratory animals from MRI data is associated with some problems. This paper proposes a method of MRI data processing which allows to eliminate the fragmentation of reconstructed vascular net. Problem of vessels fragmentation occurs in the case when vessels are parallel to the scanning plane. Our approach is based on multiple scanning, object under consideration is probed by several sets of parallel planes. The algorithm is applied to real MRI data of small laboratory animals and shows good results.

1. Introduction

In the conventional approach to reconstruction vasculatures based on MRA data, the object of interest is scanned by a series of parallel planes; the images of object slices acquired from the dataset. The imaging device registers the blood flow using the normal to section scan plane. The most informative sections are the ones with the most intense blood flow. Hence, the most informative scan, in terms of reconstructing vasculature, is the one where the set of the scan planes is perpendicular to the axes of the scanned vessels. In living organisms, however, it is impossible to choose one set of parallel planes that would be perpendicular to the axes of all blood vessels. This is due to both the various positions of the vessels and to vascular tortuosity. As a result, the reconstructed models of vasculatures contain interruptions in vessels that make these models unusable for hemodynamic studies.

The aforementioned reasons are characteristic of any study objects, but they are specifically common for studies in small laboratory animals.

In terms of mathematics, the tomographic data $A(x, y, z)$ (image intensity) is dependence

$$A(x, y, z) = F(\vec{v}(x, y, z), \vec{n}) \qquad (1)$$

from blood flow velocity vector $\vec{v}(x, y, z)$ at point (x, y, z) and normal to the scan plane vector $\vec{n}$. The function $F(\vec{v}(x, y, z), \vec{n})$ sets the image intensity value at (x, y, z) of a slice and takes small values at $(\vec{v}(x, y, z), \vec{n}) \approx 0$. There are two situations that correspond to the low image intensity in the images of slices:

1) There is no flow in the cross-section, or it is very slow: $\vec{v} \approx 0$

2) Velocity vector $\vec{v}$ and normal vector $\vec{n}$ are not collinear.

The first situation corresponds to the static tissue or thinning of a vessel (stenosis), while the second situation is caused by the specifics of the equipment and leads to the data loss. The paper deals with a technique that allows practitioners to overcome, to a certain extent, the problem of data loss, by varying the angle of the section view of a vessel at point (x, y, z).

From a mathematical point of view, the task of reconstructing the vasculature lies in defining the boundaries of a 3D area V in a way that

$$V = \{(x, y, z): A(x, y, z) > A_0\} \qquad (2)$$

where $A_0 \in \mathbb{R}-$ is a numerical value that separates the scanned environment into blood vessels and adjacent tissues based on the intensity of images acquired.

2. Scan plane slope variation technique

Description of the principle of this method. A standard scan is carried out by using a single set of parallel planes, and, as a rule, their common normal vector is parallel to the axis of the scanned object. The technique of varying the slope of the scan plane lies in the deviation of the normal vector from its "standard position" by certain angles and scanning by using more than one set of planes designed by preprogrammed normal vectors. The number of different positions of the normal vector defines the number of scan planes sets and, hence, the number of acquired datasets.

The images of vessels will appear in different intensity depending on changed positions of the scan plane. The highest image intensity is achieved by the smallest deviation of the vessel's axis from the normal to the scan plane. The subsequent analysis of the acquired datasets allows for the reconstruction of the vasculature, practically, without interruptions.

Figure 1 schematically presents the images of the object sliced by planes with different normal vectors. Vector n_1 is the normal to one of the sets of parallel planes; one specimen of this set is shown in green (together with the cross-section of the study object). Vector n_2 is the normal to another set of parallel planes; one specimen of this set is shown in red (together with the cross-section of the study object).
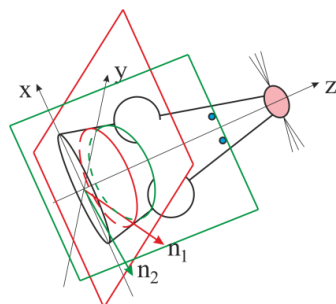

Figure 1. Cross-sections of the object made using different normal vectors

3. Steps of the vascularity reconstruction algorithm based on the method of varying the slope of the scan plane

3.1. Creating the area common for all datasets

The reasoning in this paragraph lies within the plane frame of the scanner. The authors used the imaging data recorded in DICOM format [17].

The data in each dataset is known in a 3D area in the form of a rectangular parallelepiped. The areas of different datasets are different. According to scanner specifications, each slice contains 256 rows and 256 columns. Let us express the parallelepiped containing the known data of dataset i as K_i. Construct the smallest cube K, contains the $\bigcup_{i=1}^{n} K_i$ set, that is, all parallelepipeds with known datasets.

Cube K is a "carrier" of all tomographic data at our disposal.

3.2. Interpolation of all datasets data onto a common 3D grid

Let us cover all side planes of cube K with a uniformly spaced 3D grid and find all datasets data approximation onto the 256×256×256 grid of cube K.

3.3. Combination of data from different datasets

Following the interpolation of data into the common grid area, we have a number (one array per each of datasets) of 3D arrays of the same size: B^i, $i = 1,\dots,n$, n − represents the number of available datasets. Having interpolated data from all datasets into the common grid area, we need to construct a single array containing all the information required.

3.4. Layer-by-layer pre-processing of data

MRA data has certain limitations that complicate its subsequent processing. Major limitations:
1. Inhomogeneous intensity of images (both of each given slice and across all of the slices). This effect is due to the inhomogeneity of the field in the receiver coil.
2. Layer-by-layer normalization of the reconstruction. In DICOM format, the image intensity of each given slice is scaled onto an 8- or 16-bit grid.
3. Data noise
4. Unclear boundaries of the blood flow.

These are the steps taken at the layer-by-layer data pre-processing stage.
1. Vertical alignment of the image intensity in a slice.
2. Horizontal alignment of the image intensity in a slice.
3. Adjustment of brightness and contrast settings
4. Noise reduction and image smoothing by applying the Fourier filter.

The layer-by-layer pre-processing stage allows for the reduction of some of the listed limitations.

3.5. Segmentation

For the purpose of subsequent hemodynamic calculations, the bitmap images acquired during the previous stages need to be converted into vector 3D format images, having highlighted the walls of the vessels (more precisely, the blood flow boundaries), that is, having segmented the images acquired. The segmentation is carried out in the ITK-Snap software environment [18].

3.6. Enhancement of fragmented vasculature. Local varying of segmentation parameters in small areas using the dialogue mode

As a rule, the vasculature acquired by applying the scan plane slope variation method with subsequent segmentation already contains a small number of fragments, but it may contain blood vessel interruptions. This occurs because the value set as the slicing parameter A_0 in (2) of the previous stage cannot be uniformly used across the entire image. There are areas that visually contain vessels, however, the chosen slicing parameter is too high for the vessels in these areas to be segmented.

For the purposes of segmentation, the parts of the vasculature containing interruption of a vessel are locked in subareas for which the slicing parameters are defined individually.

4. Realization of the proposed algorithm in MRI data of the mouse brain

The circulatory system of a laboratory mouse brain was chosen as an object of the study. Typically, mouse major vessels are 0.29 mm (vertebral artery). Experiments were carried out on unique scientific installation - Centre for Genetic Resources Laboratory Animals (RFMEFI61914X0005 and RFMEFI62114X0010). The field strength of the research scanner Bruker BioSpec 117/16USR used by the authors to acquire data presented in this paper - 11.7 T. For scanning, the "1H mouse brain surface coil" RF coil is used.

4.1. Tomography data details

Each data set contains 256 DICOM images of slices with associated metadata. All images are bitmaps in the shades of gray that are expressed by a 256 rows x 256 column square matrix. The reconstruction is carried out within cube *K* with an edge length of 24.9 mm.

4.2. Single dataset reconstruction

Reconstructing the mouse brain vasculature based on the data acquired by the standard scanning technique, the resulting vasculature following the main segmentation stage consists of 18 fragments. This vasculature is shown in figure 2.
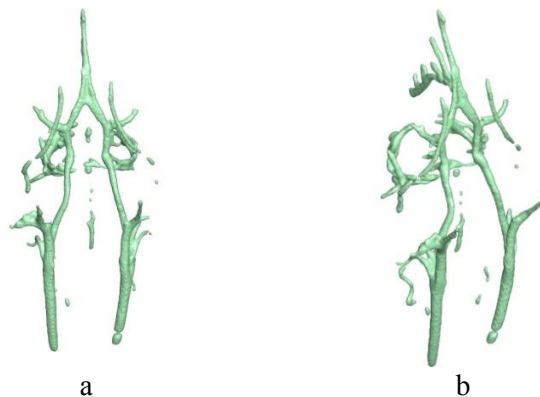

a   b

Figure 2. Vasculature reconstructed based on the standard image acquisition technique in frontal view (a), turned at a 45- degree angle around longitudinal axis (b).

The resulting vasculature is marked by the pronounced fragmentation of vessels, and the missing fragments are quite large. This kind of vasculature cannot be used, neither in morphological studies, or in modelling the blood flow.

4.3. Reconstruction based on combined data from five datasets

Let us reconstruct the vasculature using the data acquired in the layer-by-layer pre-processing of the five datasets and their subsequent combination as the basis for segmentation. Following the segmentation, we acquire the vasculature consisting of 12 fragments (figure 3).

Notwithstanding the fact that this vasculature still lacks integrity, it is still more informative that above. We can see longer runs of vessels that have only local interruptions.
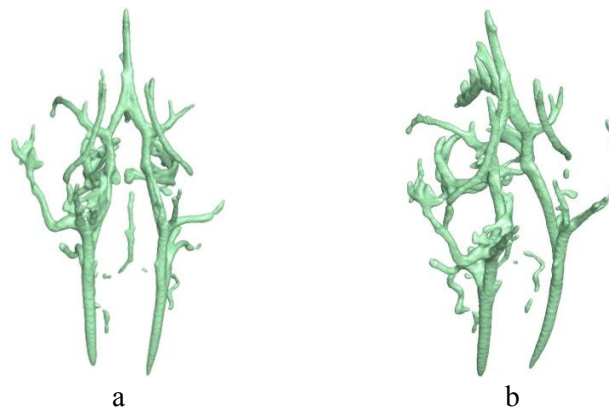
a   b

Figure 3. Vasculature reconstructed based on the data from five datasets: in Willis's circle view (a); and as rotated (b).

4.4. Reconstruction based on the combined data from five datasets with subsequent enhancement using the dialogue mode

Having enhanced the vasculature described above (figure 3) using the dialogue mode, we have acquired the vasculature consisting of 2 fragments (figure 4).
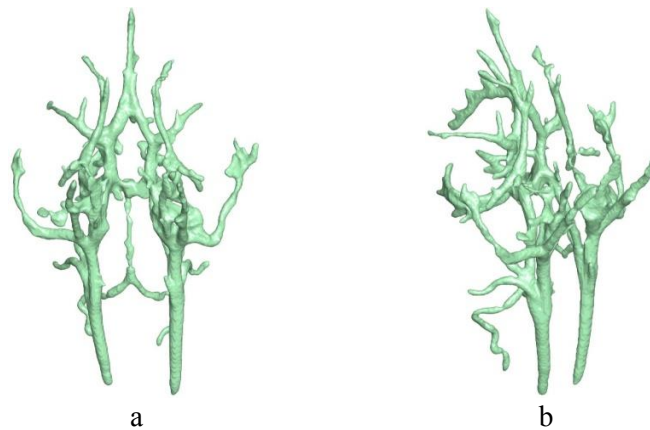

a   b

Figure 4. The vasculature acquired based on the data from five datasets that was subsequently enhanced in the dialogue mode: in Willis' circle view (a), and as rotated (b).

This vasculature can be used for the modelling of the mouse brain blood flow.

5. Conclusion

The algorithm proposed allows for the reconstruction of the one-fragmental vascularity of mouse and rat brains. The resulting vasculature model as compared to the model reconstructed based on a single scan data, offers the following advantages:

1. It shows vessels that do not visualize in the model reconstructed based on a single scan.
2. It has less number of fragments than the single scan based model.

However, the acquired 3D model of the mouse brain vascularity has a number of drawbacks, and namely: somewhat increased diameter of the vessels; perivascular cerebrospinal fluid spaces are visualized.

The main disadvantage of our method is of course time consuming. The acquiring of each additional data package takes the same time as the standard one. Sure this fact decreases the method

significance for medical applications. But in preclinical and biological researches (when time consuming is not so important) it may be successfully applied. Also our many-packages method require additional time as averaging and may replace that in some cases.

The task of reconstructing a volumetric vasculature of complex branched geometry is required in many applications (medicine, neurobiology); it is also a matter of interest for MRA practitioners. The currently available technique sallow for a limited realization of this task in terms of both its scope and quality. This task is closely related to the classic problem of vector tomography in reconstruction of a 3D vector based on the acquired imaging data. The proposed algorithm of varying the slope of the scan plane allows for the reconstruction of branched vasculatures and solves the problem of fragmented vessels in MRA data based models. The examples where the algorithm was used to reconstruct actual brain vasculatures in small laboratory animals, prove, beyond doubt, the efficiency of this method and demonstrate the associated advantages, and namely: significant decrease of fragmentation in the reconstructed vasculature and visualization of vessels that remain unseen using the standard reconstruction technique.

The advantages of the proposed algorithm give ground for its successful application in processing MRA data for its subsequent use in hemodynamic studies and phenotyping of genetic lines of laboratory animals with vascular pathologies.

References
[1]   Grist T M, Mistretta C A, Strother C M and Turski P A 2012 Time-resolved angiography: Past, present, and future *J. Magn. Reson. Imaging.* **36 (6)** 1273-86
[2]   Beckmann N 2000 High resolution magnetic resonance angiography non-invasively reveals mouse strain differences in the cerebrovascular anatomy in vivo *Magn Reson Med* **44 (2)** 252-8
[3]   Vorobtsova N A, Yanchenko A A, Cherevko A A, Chupakhin A P, Krivoshapkin A L, Orlov K Yu, Panarin V A and Baranov V I 2013 Modelling of cerebral aneurysm parameters under stent installation *RJNAMM* **28 (5)** 505-516
[4]   Yanchenko A A, Cherevko A A, Chupakhin A P, Krivoshapkin A L and Orlov K Yu 2014 Nonstationary hemodynamics modelling in a cerebral aneurysm of a blood vessel *RJNAMM* **29 (5)** 307-317
[5]   Miraux S, Franconi J M and Thiaudie`re E 2006 Blood Velocity Assessment Using 3D Bright-Blood Time Resolved Magnetic Resonance Angiography *Magn Reson Med* **56** 469-473
[6]   Angenent S, Pichon E and Tennenbaum A 2006 Mathematical methods in medical image processing *Bulletin AMS* **43 (3)** 365-396
[7]   Alvarez L, Guichard F, Lions P L and Morel J-M 1993 Axioms and fundamental equations of image processing *Arch. Rat. Mech. Anal.* **3** 199-257
[8]   Alvarez L, Lions P L and Morel J-M 1992 Image selective smoothing and edge detection by nonlinear diffusion *SIAM J. Numer. Anal.* **29** 845-866
[9]   Koenderink J J 1984 The structure of images *Biological Cybernetics* **50** 363-370
[10]   Perona P and Malik J 1990 Scale-space and edge detection using anisotropic diffusion, *IEEE Trans. Pattern Anal. Mach. Intell.* **12** 629-639
[11]   Roberts L 1965 Optical and electro-optical information processing, ch. Machine perception of

       3-D solids. *MIT Press*

[12] Sobel I E 1970 *Camera models and machine perception* (Ph.D. thesis, Stanford Univ.)

[13] Witkin A, Kass M and Terzopoulos D 1987 Snakes: active contour models *Int. Journal of Computer Vision* **1** 321-331

[14] Casselles V, Catte F, Coll T and Dibos F 1993 A geometric model for active contours in image processing *Numerische Mathematic* **66** 1-31

[15] Sethian J, Malladi R and Vemuri B 1995 Shape modeling with front propagation: a level set approach *IEEE Trans. Pattern Anal. Mach. Intell.* **17** 158-175

[16] Morel J-M and Solimini S 1995 Variational methods in image segmentation *Birkhauser, Boston*

[17] http://medical.nema.org

[18] Yushkevich P A, Piven J, Hazlett H C, Smith R G, Ho S, Gee Js C and Gerig G 2006 User-guided 3D active contour segmentation of anatomical structures: Signi_cantly improved efficiency and reliability *Neuroimage* **31 (3)** 1116-28